

## Broadband coherent radiation based on peculiar multiple Raman scattering by laser-induced phonon gratings in TiO<sub>2</sub>

Kuon Inoue,<sup>1,2,\*</sup> Jun Kato,<sup>1</sup> Eiichi Hanamura,<sup>1</sup> Hayato Matsuki,<sup>1</sup> and Eiichi Matsubara<sup>3</sup>

<sup>1</sup>Chitose Institute of Science and Technology, 758-65 Bibi, Chitose 066-8655, Japan

<sup>2</sup>Toyota Physical and Chemical Research Institute, Nagakute, Aichi 480-1192, Japan

<sup>3</sup>Graduate School of Engineering, Hokkaido University, Sapporo 060-8626, Japan

(Received 24 January 2007; revised manuscript received 2 May 2007; published 2 July 2007)

We have found in TiO<sub>2</sub> broadband coherent anti-Stokes Raman scatterings in unusual origin by exciting a pair of optical phonons with the use of crossed beams of two-color subpicosecond pulses. Angle-resolved spectroscopy reveals that the spectral lines up to the 22nd-order with nearly equal scattering-angle separation appear with their intensities of the same order; the conventional phase matching is not satisfied. Formation of a standing-wave type phonon grating is responsible for the signals. Application of this phenomenon to developing ultrafast optical pulses is discussed.

DOI: [10.1103/PhysRevB.76.041101](https://doi.org/10.1103/PhysRevB.76.041101)

PACS number(s): 42.65.Dr, 63.20.Dj

Generation of high-order stimulated Raman scattering (SRS) is one of the most interesting nonlinear-optical phenomena and has been extensively studied in physics and from the application point of view. In the 1970s high-order coherent anti-Stokes Raman scattering (CARS) by vibration modes in molecular gases such as H<sub>2</sub> was considered to be a powerful means of providing a wavelength-variable coherent light source in the ultraviolet region. In the 1980s, a resonant pumping method using two-color lasers with their frequency difference tuned to Raman transition was introduced to efficiently induce the high-order CARS signals.<sup>1</sup> In the 1990s, a concept of maximal Raman coherence, which is attained under quasiresonance, was introduced<sup>2</sup> and has been utilized to adiabatically generate a broadband coherent spectrum consisting of equidistant frequency spectral lines.<sup>3</sup>

Currently, producing ultrashort light pulses including subfemtosecond ones is an important issue in quantum optics.<sup>4,5</sup> That those pulses would provide a spectroscopic method on an even shorter time scale than several femtoseconds should be of great significance in both fundamental and applied sciences. For this purpose, we need to obtain a broadband phase-coherent spectrum, from which the synthesis of ultrashort pulses is possible by Fourier transformation. A few methods of generating such a spectrum have been proposed, but the high-order SRS<sup>6,7</sup> has an advantage in that the conversion efficiency is high over other methods such as high-order harmonic generation.<sup>8</sup> So, in the last decade the high-order SRS phenomenon has been intensively studied in molecular gas systems with the exception of solid hydrogen.<sup>9</sup> This is because in gases the phase-matching (PM) condition can be satisfied rather easily up to high-order signals. Since a quantity of the oscillator strength times the number of oscillator per unit volume is small in gases because of low density, a collinear two-color pumping has been employed in most cases, together with a long sample cell for efficient light-matter coupling. In this connection, the SRS due to an optical phonon (vibrational Bloch state) in condensed matter should be apparently attractive because the corresponding quantity or the coupling strength is much stronger compared to gaseous systems. This is partly because the effective number of oscillator per unit volume is much larger in condensed

matters, and partly because the phonon is an elementary excitation being coherent over many unit cells.

In this Rapid Communication, we report on the generation of peculiar multiple CARS signals due to optical phonons in a rutile crystal (TiO<sub>2</sub>). This observation of broadband radiation is made possible using crossed beams of two-color subpicosecond-pulse lasers for resonant excitation of a two-phonon state.<sup>10</sup> Taking full advantage of angle-resolved spectroscopy we find that the signals up to very high order appear with nearly equal scattering-angle separation like the “Raman-Nath” scattering (hereafter we call the present phenomenon the RN-like one). Those spectral lines are explained as arising from multiple scatterings of one incident laser by a pair of “gratings” of the phonons that condense themselves at the  $\Gamma$  point after moving from the Brillouin-zone (BZ) edges due to BZ folding.<sup>10</sup> A standing-wave type of phonon grating with a periodicity created along the particular direction due to condensation is responsible for the RN-like signals.

TiO<sub>2</sub> belongs to the structure of  $D_{4h}$  symmetry with inversion symmetry. There are 15 optical phonons at the  $\Gamma$  point. Four modes among them are Raman ( $R$ ) active. Their  $R$ -tensors are such that  $R(A_{1g})=[\alpha_{aa}+\alpha_{bb}, \alpha_{cc}]$ ,  $R(B_{1g})=[\alpha_{aa}-\alpha_{bb}]$ ,  $R(B_{2g})=[\alpha_{ab}]$ , and  $R(E_g)=[(\alpha_{bc}, \alpha_{ac})]$ , where  $a$ ,  $b$ , and  $c$  are the crystallographic axes with  $a$  and  $b$  symmetric.<sup>11</sup> Based on the observed  $R$ -spectra, we reconfirmed that the respective frequencies of the  $B_{1g}$ ,  $E_g$ ,  $A_{1g}$ , and  $B_{2g}$  modes are 143, 447, 612, and 826 cm<sup>-1</sup>.<sup>12</sup> For later use, we mention the spectrum observed in  $a(b,b)c$  geometry, showing three spectral lines with the frequency shift of 143, 612, and 230 cm<sup>-1</sup>; the broad spectrum of 230 cm<sup>-1</sup> is the second-order signal. It is noted that strong second-order RS signals are also distributed continuously over 150–730 cm<sup>-1</sup> as the background.

Two 0.5-mm-thick plate samples ( $c$ - and  $a$ -cut) with planes of  $8.0 \times 8.0$  mm<sup>2</sup> in area were used. Two laser pulses of 150 fs in pulse duration having near-infrared angular frequency and wave vectors of  $(\omega_1, \mathbf{k}_1^0)$  and  $(\omega_2, \mathbf{k}_2^0)$ , respectively, were employed to resonantly excite either a two-phonon state at the BZ edges or a one-phonon state at the  $\Gamma$  point. Signal and idler output beams from an optical para-

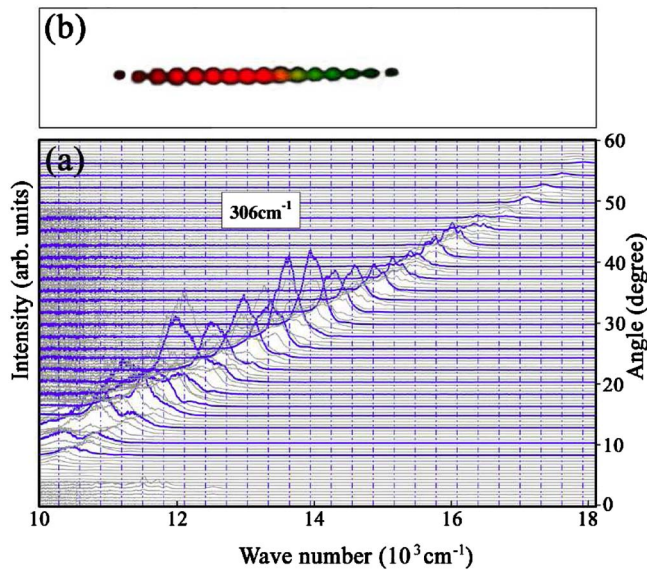


FIG. 1. (Color online) (a) Angle-resolved Raman-Nath-like CARS spectra in  $\text{TiO}_2$ , excited by two lasers; their frequency and energy are  $\omega_1=6562 \text{ cm}^{-1}$  and  $9.8 \mu\text{J/pulse}$  and  $\omega_2=5955 \text{ cm}^{-1}$  and  $10.0 \mu\text{J/pulse}$ . The spectrum is observed at every  $0.5^\circ$ . (b) A photograph of the scattered-light spots on a screen.

metric amplifier (OPA) pumped by a regeneratively amplified mode-locked Ti-sapphire laser were used as  $\omega_1$  and  $\omega_2$  pulses, respectively.<sup>10</sup> Two crossed beams with a small angle  $\Delta\theta$  of  $\sim 4.5^\circ$  in air were focused onto a sample using a lens with a focal length of 150 mm. The power density up to  $2 \times 10^{11} \text{ W/cm}^2$  was employed. The polarizations of two lasers were parallel to the  $b$  axis of the sample, so that the  $A_{1g}$  and  $B_{1g}$  modes can be excited. The scattered radiation was picked up with an optical fiber head with a window of 3 mm in height and 0.5 mm in width. The head attached to an electrically movable rotation stage was set about 25 mm apart from the sample, and thereby, angle-resolved spectra could be observed; actually, the CARS spectra were measured at every  $0.5^\circ(0.2^\circ)$  in the visible (near-infrared) region from 400 to 1000 nm (900 to 1600 nm) in wavelength. The signal radiation was detected with a spectrometer (Ocean Optics Inc., HR2000) with a one-dimensional (1D) arrayed charge coupled device (CCD) detector. In the near-infrared region a monochromator with a cooled 1D arrayed InGaAs detector was employed.

Figure 1(a) shows an example of a series of angle-resolved “visible” spectra for an  $a$ -cut sample. For later use, we define  $x$ ,  $y$ , and  $z$  axes to be parallel to the  $c$  axis, the  $-b$  axis, and the normal of the plate ( $a$ -cut), respectively, so that the  $x$  axis is in the plane formed by  $\mathbf{k}_1$  and  $\mathbf{k}_2$  with  $\mathbf{k}_1$  ( $\mathbf{k}_2$ ) being the wave vector in the sample corresponding to  $\mathbf{k}_1^0$  ( $\mathbf{k}_2^0$ );  $\Delta\omega=\omega_1-\omega_2$  was chosen to be nearly  $612 \text{ cm}^{-1}$ , which is the frequency of the  $A_{1g}$  phonon. It is seen in Fig. 1(a) that a series of spectral lines manifest themselves in such a manner as the frequency and angle differences between the adjacent signals are almost constant, i.e.,  $306 \text{ cm}^{-1}$  and  $2.0^\circ$ , respectively. Using a camera, we also took a photograph of signal light spots on a screen placed behind the sample. It is presented in Fig. 1(b), where 15 light spots appear. Notice

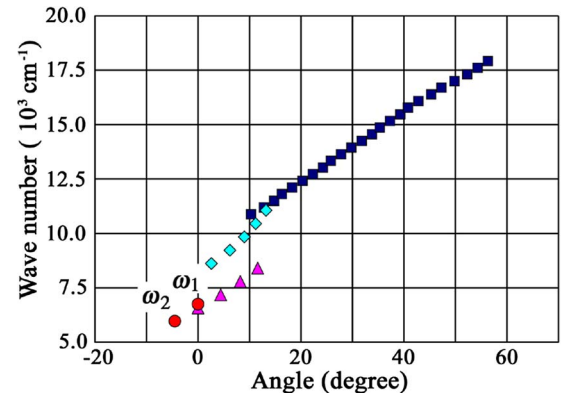


FIG. 2. (Color online) A plot of  $\omega_{ob}$  vs  $\theta_{ob}$  (scattered angle) for Raman-Nath-like signals (squares); triangle and diamond denote the PM-CARS signal due to the  $A_{1g}$  phonon and spectral lines of unknown origin in the near-infrared region, respectively, and two circles refer to the incident beams.

that the feature of the equidistant angle is also recognized among the spots. Importantly the value of  $306 \text{ cm}^{-1}$  does not correspond to any frequency of four  $R$ -active phonons at the  $\Gamma$  point, but to that of  $305 \text{ cm}^{-1}$  of the phonons at the  $X$  point of the BZ edge. The observed feature of both the equal frequency- and angle-separations formally resembles that of the so-called RN signals,<sup>13</sup> although the physics differs essentially from each other. Another noticeable feature in Fig. 1(a) is that the spectral intensity does not monotonously decrease as the order is higher, and on the contrary, it becomes maximum for some spectral line around the middle of the series. The corresponding “near-infrared” spectra (not shown) are not so simple compared to those in the visible region.

A plot of the signal frequency  $\omega_{ob}$  vs the observed angle  $\theta_{ob}$  is presented in Fig. 2 where a few “near-infrared” data are also included; notice that the RN-like signals of the lower orders are missing. We also estimated experimentally each RN-like-signal intensity relative to that of the transmitted  $\omega_1$ -laser. A total conversion efficiency  $\eta$  to all the RN-like signals is 2% to 3% in this case.

Let us elucidate the generation mechanism of the present signals. First we explain where the phonon of  $306 \text{ cm}^{-1}$  arises from; note that there is no  $\Gamma$ -point phonon with a frequency in a range from 189 to  $370 \text{ cm}^{-1}$ . In addition to the  $A_{1g}$   $\Gamma$  phonon of  $612 \text{ cm}^{-1}$ , two  $X_1$ -phonon modes each with a frequency  $\omega_{ph}$  of  $305 \text{ cm}^{-1}$  at the opposite  $X$  points can be coherently driven by the induced  $R$  scattering.<sup>14</sup> As a result, a dynamical grating of the two-phonon complex is formed with  $\mathbf{k}_{ex}=\mathbf{k}_1-\mathbf{k}_2$ . The phase of two phonons (vibrations) with the respective wave vectors of  $(\mathbf{G}_X/2)+\mathbf{k}_{ex}/2$  and  $-(\mathbf{G}_X/2)+\mathbf{k}_{ex}/2$ , where  $\mathbf{G}_X$  is the reciprocal lattice vector parallel to the present  $z$  axis, differs by  $\pi$  in two neighboring unit cells and the unit-cell size is doubled in the “ $z$ ” direction for those phonons. This implies that the  $\pm X$  points at BZ edges are folded onto the  $\Gamma$  point, and those phonons should condense themselves temporarily.<sup>10</sup> Under this dynamical symmetry breaking, two single- $X_1$  phonons of  $D_{4h}$  are reduced to  $A_{1g}$ ,  $B_{1g}$ , and  $B_{2g}$  modes at the  $\Gamma$  point of  $D_{2h}$ ,

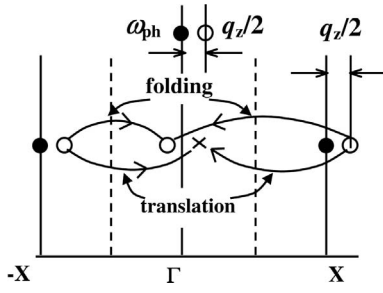


FIG. 3. Illustration showing how a pair of  $X_1$  phonons originally around BZ edges ( $\pm X$  points) move to the vicinity of the  $\Gamma$  point because of folding and translation symmetry.

which are all  $R$ -active. In the present  $(b, b)$  polarization, both  $A_{1g}$  and  $B_{1g}$  phonons are possible to generate CARS signals. Because of the folding and newly acquired translational symmetry of  $G_X/2$  (see Fig. 3), the “ $z$ ”-wave-vector component of those phonons becomes such that one is  $(k_{ex})_z/2$ , and the other,  $-(k_{ex})_z/2$ , with the common  $x$  component. As a result, a phonon grating of standing-wave type with a periodicity of  $(2\pi k_z^{ex}/2)^{-1}$  is formed in the  $z$  direction, which plays an essential role in generating the RN-like signals.

Let us first consider a simpler case where the  $\Gamma$  phonon ( $A_g$ ) with  $\omega_{ph}=612\text{ cm}^{-1}$  is coherently excited. In this case, only one phonon “grating” of traveling-wave type is formed. Therefore a series of CARS signals due to successive scattering of the  $\omega_1$ -light by the grating are supposed to appear. If the quasi-PM condition is satisfied, the  $l$ th-order anti-Stokes signals should appear at  $\omega_{+l}=\omega_1+l\omega_{ph}$  in the direction along  $k_{+l}=k_1+lq$  with  $q=k_{ex}$ ; note that the angle  $\delta\theta_l$  between the  $(l+1)$ th and  $l$ th signals becomes smaller with increasing  $l$ , since  $k_{+l}$  is larger. Actually, a few  $l$ th states with small  $l$  satisfying the relation  $\Delta k \leq L^{-1}$  can radiate;  $\Delta k$  and  $L$  are the phase mismatch and the effective sample thickness, respectively;  $\Delta k$  increases with increasing  $l$  (see Fig. 4). The

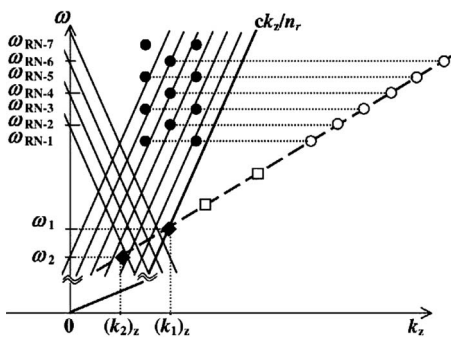


FIG. 4. A schematic showing how a series of Raman-Nath-like signals radiate from a radiation point close to the light cones (thin lines) shifted by multiples of the periodicity from the original one,  $ck/n_r(\omega)$ , where  $c$  and  $k$  are the velocity and wave vector of light in air, respectively, and  $n_r$  is the refractive index of  $\text{TiO}_2$ . Radiation is allowed to emit only from a point on or close to the light cone. Radiation points (open circles) on the thick (long dashed) line move to different ones (closed circles) by scatterings due to phonon gratings; the line is such that the points on it satisfy the relevant wave-vector conservation relation.

number of such radiations depends on  $\Delta\theta^0$ .

Now the situation for a pair of phonon gratings differs completely from the above. Multiple scatterings by both the phonon gratings with the  $+z$  and  $-z$  components lead the  $\omega_1$  light to a radiation point very close to the light cone, as is schematically shown in Fig. 4; notice that the frequencies of both gratings are the same. It is important to note that the shifted version of the original light cone by  $h \cdot (k_z^{ex}/2)$  along the  $\pm z$  also serves as the light cone, because of the periodicity of  $(\pi k_z^{ex})$ ;  $h$  is any integer. More specifically, as the result of  $m$ -times scatterings by the grating with the  $+z$  component and  $n$ -times scatterings by that with the  $-z$  component, the  $\omega_1$  light is scattered to a radiation state with the frequency of  $(m+n)\omega_{ph}$  and the wave vector of  $[(m+n)(k_x^{ex}/2), 0, (k_1)_z + (m-n)(k_z^{ex})/2]$ , where  $m$  and  $n$  are either the positive integer or 0. Since  $m=n$  or  $n \pm 1$  is most likely the case,  $l$ -times scatterings with  $l=m+n$  cause the  $l$ th-order CARS signal to radiate in the direction  $\theta_{+l}^{RN}$

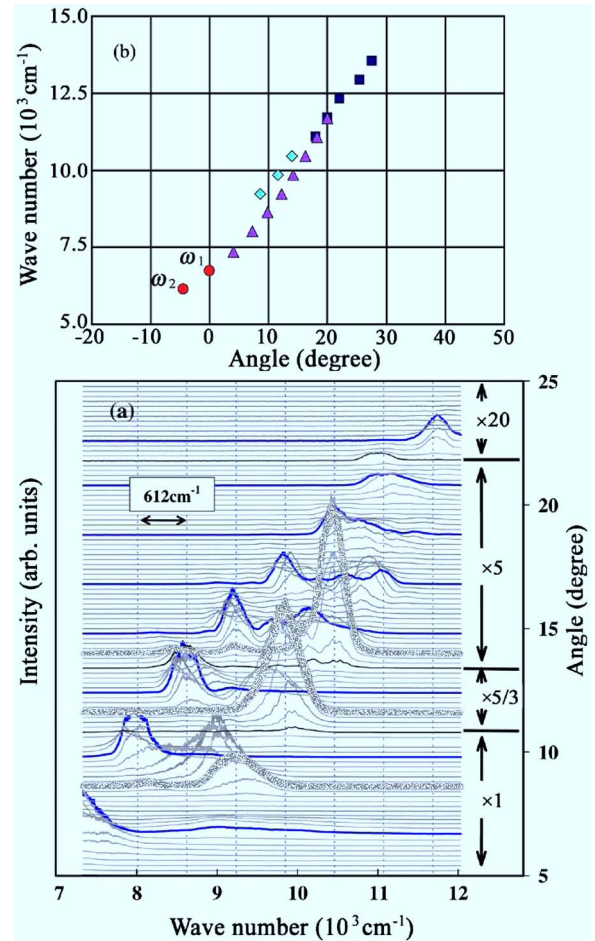


FIG. 5. (Color online) (a) Another example of angle-resolved CARS spectra in the near-infrared region in  $\text{TiO}_2$ , observed under a condition slightly different from that in Fig. 1(a). In this case the Raman-Nath-like spectra with  $306\text{ cm}^{-1}$  separation are not clearly observed in the visible region. The dense black and thick gray lines denote the CARS spectrum and the spectrum in unknown origin, respectively. (b) A plot of  $\omega_{ob}$  vs  $\theta_{ob}$  for (a), the same symbols are used as in Fig. 2.



$=\tan^{-1}[l(k_x^{ex}/2)/k_z] \cong l(k_x^{ex}/2)/k_z$ , so long as  $l(k_x^{ex}/2)/k_z$  is small, where  $k_z$  is either  $(k_1)_z$  or  $(k_1)_z \pm (k_z^{ex}/2)$ . From this it follows that the RN-like scattering with almost equal angle separation should be observed.

Let us discuss the result. First, in Fig. 1(a) the signals are actually observed at  $\omega_{+l} = \omega_1 + \omega_{in} + l\omega_{ph}$  in the direction along  $\mathbf{k} = (k_{1x} + k_{in} + lq_x, 0, k_{1z})$  with unknown constant values  $\omega_{in}$  and  $k_{in}$  (see Fig. 2). At present, the reason is not necessarily clear to us. Second, we mention that how high orders of signals can be observed depends on the relative focusing positions and time delay between two incident pulses. This is also the case with  $\eta$ . In some cases, more than 10% is reached as a total value of  $\eta$  with almost the same incident powers.

Third, we mention briefly the result for the quasi-PM case; typically, a few PM signals are observed in addition to the RN-like ones. Figure 5(a) shows such an example of the angle-resolved spectra, which were observed with the relative focusing points of two incident pulses different from the case of Fig. 1(a), but with otherwise the same experimental condition. Figure 5(b) shows a plot of  $\omega_{ob}$  vs  $\theta_{ob}$ , including the “visible” data (the spectra are not shown). Anti-Stokes signals with an equidistant frequency  $612 \text{ cm}^{-1}$  of a *R*-active phonon from the first to eleventh order are observed,<sup>15</sup> the visible spectra observed up to  $14\,000 \text{ cm}^{-1}$  at most are so complicated that it is not clear whether the RN-like signals with a  $306 \text{ cm}^{-1}$  separation appear or not. The observed angles [see Fig. 5(b)] reveal that the quasi-PM condition is

well-satisfied up to the eighth-order signal. An  $\eta$  value to the PM signals amounts to almost 50%.

Finally, the present RN-like phenomenon is considered to provide a promising means of generating ultrashort optical pulses because the signals are coherent with each other. A problem is how all the signals can be made collinear, which is required to make those Fourier transformed. This should be possible using an appropriate compensator. Suppose this is done for the present RN-like spectra, extending roughly from  $10\,000$  to  $17\,000 \text{ cm}^{-1}$  with a continuous background. Fourier transformation of this spectrum should generate an ultrashort pulse of 5 fs in duration. Owing to the continuous background, these short pulses are well-separated in time with each other,<sup>16</sup> so that they should be useful in an ultrafast spectroscopy. There is the possibility of extending the spectrum to the very ultraviolet region using a crystal with a large band gap such as BN and diamond.

In summary, we have observed broadband multiple Raman-Nath-like CARS signals in a  $\text{TiO}_2$ , which are induced by crossed beams of two-color lasers. Angle-resolved spectroscopy reveals that the signals up to the 22nd order appear with a nearly equal scattering-angle separation. We find that a standing-wave type phonon grating is responsible for the present peculiar signals.

We are grateful to Y. Tanabe of University of Tokyo for valuable discussions.

\*inoue@guppy.chitose.ac.jp

<sup>1</sup>T. Imasaka, S. Kawasaki, and N. Ishibashi, *Appl. Phys. B: Photophys. Laser Chem.* **49**, 389 (1989).

<sup>2</sup>S. E. Harris and A. V. Sokolov, *Phys. Rev. A* **55**, R4019 (1997); *Phys. Rev. Lett.* **81**, 2894 (1998).

<sup>3</sup>A. V. Sokolov, D. R. Walker, D. D. Yavuz, G. Y. Yin, and S. E. Harris, *Phys. Rev. Lett.* **85**, 562 (2000).

<sup>4</sup>P. Tzallas, D. Charalambidis, N. A. Papadoqiannis, K. Witte, and G. D. Tsakiris, *Nature (London)* **426**, 267 (2003).

<sup>5</sup>M. Y. Shverdin, D. R. Walker, D. D. Yavuz, G. Y. Yin, and S. E. Harris, *Phys. Rev. Lett.* **94**, 033904 (2005).

<sup>6</sup>M. Wittmann, A. Nazarkin, and G. Korn, *Phys. Rev. Lett.* **84**, 5508 (2000).

<sup>7</sup>E. Sali, P. K. Kinsler, G. H. C. New, K. J. Mendham, T. Halfmann, J. W. G. Tisch, and J. P. Marango, *Phys. Rev. A* **72**, 013813 (2005).

<sup>8</sup>T. Brabec and F. Krausz, *Rev. Mod. Phys.* **72**, 545 (2000).

<sup>9</sup>J. Q. Liang, M. Katsuragawa, F. Le Klein, and K. Hakuta, *Phys. Rev. Lett.* **85**, 2474 (2000).

<sup>10</sup>E. Matsubara, K. Inoue, and E. Hanamura, *Phys. Rev. B* **72**, 134101 (2005).

<sup>11</sup>R. Loudon, *Adv. Phys.* **13**, 423 (1964).

<sup>12</sup>S. P. Porto, P. A. Fleury, and T. C. Damen, *Phys. Rev.* **154**, 522 (1967).

<sup>13</sup>M. Born and E. Wolf. *Principles of Optics*, 7th ed. (Cambridge University Press, Cambridge, England, 1999), Chap. XII.

<sup>14</sup>J. G. Traylor, H. G. Smith, R. M. Nicklow, and M. K. Wilkinson, *Phys. Rev. B* **3**, 3457 (1971).

<sup>15</sup>H. Matsuki, K. Inoue, and E. Hanamura, *Phys. Rev. B* **75**, 024102 (2007).

<sup>16</sup>E. Matsubara, K. Yamane, T. Sekikawa, and M. Yamashita, *J. Opt. Soc. Am. B* **24**, 985 (2007).